THE ASTROPHYSICAL JOURNAL, 367:126–140, 1991 January 20

STELLAR POPULATION SYNTHESIS REVISITED

STÉPHANE CHARLOT
Space Telescope Science Institute; and Département d'Astrophysique Extragalactique et de Cosmologie, Observatoire de Paris and Université Paris VII
AND
GUSTAVO BRUZUAL A.
Centro de Investigaciones de Astronomía, Mérida, Venezuela
Received 1990 June 11; accepted 1990 July 17

ABSTRACT

We introduce a model of stellar population synthesis whose main attributes are the method used to compute the distribution of stars in the theoretical color-magnitude diagram (CMD) and the updated stellar library. Existing galaxy synthesis models are limited by their derivations of approximate isochrones in the CMD. Conventional population synthesis (by Tinsley, Bruzual, Guiderdoni and Rocca-Volmerange) cannot be used reliably to study stellar systems forming on short ($\ll 1$ Gyr) time scales. Alternatively, models that use the fuel consumption theorem (Renzini, Renzini and Buzzoni) hide approximations whose consequences on the integrated properties of stellar systems have never been properly evaluated. We circumvent the inconvenience of these techniques by developing a method of isochrone synthesis inspired from studies of the ages and colors of globular clusters. We optimize our models by compiling a library of stellar evolutionary tracks (for solar metallicity) which relies on updated stellar calculations. To limit uncertainties, we determine semi-empirically the positions in the theoretical CMD of stars on the late asymptotic giant branch (AGB).

After comparing our isochrone synthesis models with models based on the fuel consumption theorem and computed with the same library of tracks, we conclude that the latter are a reasonable although misleading approximation of population synthesis. Earlier results derived with the fuel consumption theorem (Renzini and Buzzoni) are superseded by the new library of tracks. Our isochrone synthesis models reproduce well the fractional contribution of bright AGB stars to the bolometric light of a burst population as observed in the Magellanic Clouds star clusters. We analyze the contribution of each stellar evolutionary stage to the integrated *UBVRIJKL* light of populations with various star formation laws and the Salpeter initial mass function (IMF). The resulting colors from the UV to the near-IR reproduce well the integrated colors of young (0.01–4 Gyr) star clusters in the Large Magellanic Cloud (LMC) and of present-day galaxies of various morphological types. We consider these successful comparisons of the models with observed stellar populations in a wide range of ages (from a few times 10^7 yr to a Hubble time) as an evidence for the appropriateness of the set of evolutionary tracks and of the isochrone synthesis method.

Subject headings: galaxies: evolution — galaxies: photometry — galaxies: stellar content — stars: evolution

I. INTRODUCTION

Evolutionary population synthesis has become a standard technique to study the spectrophotometric evolution of galaxies (Tinsley 1980; Bruzual 1983; Arimoto and Yoshii 1986; Guiderdoni and Rocca-Volmerange 1987). The primary goal of population synthesis models is to compute the time-dependent distribution of stars of various masses in the theoretical CMD. Once this distribution is known, the integrated spectrum of the stellar population can be inferred by adding up the spectra of individual stars. Most generally, stellar calculations provide the tracks followed in the theoretical CMD by aging stars of various masses and metallicities. Observations of nearby stars (for solar-metallicity models) or model atmospheres can then be used to assign a spectrum to a star of known temperature and luminosity. The quality of a population synthesis model therefore relies primarily on the quality and completeness of the stellar data it uses. Unfortunately, the libraries of evolutionary tracks used in existing models (Tinsley 1980; Bruzual 1983; Renzini and Buzzoni 1986; Arimoto and Yoshii 1986; Guiderdoni and Rocca-Volmerange 1987) are either incomplete or they have been assembled by patching together tracks computed by many (commonly more than five or six) different authors which used different input physics. Furthermore, the stellar evolution theory is at the present time unable to provide accurate models for the luminous pulsating stars on the upper AGB. Population synthesis models that do include these stars follow the prescriptions of Renzini and Voli (1981) which largely overestimate their importance (e.g., Frogel, Mould, and Blanco 1990 and references therein). Given the recent improvements in our understanding of stellar evolution (e.g., Bertelli *et al.* 1985; Maeder and Meynet 1989, hereafter MM) and the large quantity of data collected on AGB stars (Herman and Habing 1985; Herman, Burger, and Phennix 1986), it is now possible to put together a library of tracks in good agreement with the observations.

Regardless of the stellar input physics, population synthesis models also differ in the way their authors compute the distribution of stars in the theoretical CMD. In general, all the existing models compute *approximate* isochrones from the available set of evolutionary tracks. In conventional population synthesis (Tinsley 1980; Bruzual 1983; Guiderdoni and Rocca-Volmerange 1987) stars are binned in mass so that each mass bin is rigidly assigned to a fixed evolutionary track. At a given age, stars in a given mass bin populate a segment on their track whose length is determined by the star age dispersion, and in turn by the star formation time scale. Thus, the CMD of

the population at that age is approximated by the collection of segments populated by stars on the finite number of tracks. For time scales of star formation larger than $\gtrsim 1$ Gyr (i.e. larger than the duration of the longest stages on the tracks) the age dispersion is large enough for stars to be found at any time in several consecutive stages along the tracks. The photometric properties of the stellar population vary then smoothly in time. The formation and evolution of galaxies on shorter time scales, however, has recently been recognized as a key cosmological issue (Chambers and Charlot 1990). Also, we are facing fundamental problems in interpreting the observational features of the so-called starburst galaxies, in which the young component of the stellar population is commonly less than a few times 10^7 yr old (Joseph 1990). In the limit of short star formation time scales, all stars have nearly the same age. Thus, in conventional models of population synthesis all stars in a given mass bin populate only one evolutionary stage on their track. The computed colors and magnitudes of the population change abruptly as stars suddenly "jump" into a different evolutionary stage. Artifical *a posteriori* smoothing is therefore required in the photometric evolution of the stellar population.

Alternatively, the fuel consumption theorem (Renzini 1981) makes possible the study of arbitrarily short bursts. The theorem states that "the contribution of stars in any post–main-sequence evolutionary stage to the integrated bolometric luminosity of a burst stellar population is proportional to the amount of nuclear fuel burnt by the stars during that stage." The fuel consumption theorem has been used to model the bolometric and photometric evolution of stellar populations (Renzini 1981; Renzini and Buzzoni 1983, 1986; Buzzoni 1990 who improved the approach). However, these models usually assume that for a burst population, a given isochrone can be approximated beyond the main sequence by the evolutionary track of the current turn-off mass. In general, it is also assumed that all evolved stars have the IMF weight of the turnoff mass. Although the few predictions made with models based on the fuel consumption theorem (Renzini and Buzzoni 1986) have been contradicted by observations of star clusters (e.g., Frogel *et al.* 1990), the discrepancy was probably due to the set of tracks used (Renzini 1988). Yet, there has never been a clear analysis of the errors introduced by the approximations coupled with the fuel consumption theorem when studying stellar populations. Ironically, conventional population synthesis models do not provide a mean to do so since they cannot reliably handle star bursts.

In this paper, we develop a population synthesis method which allows us to determine more accurately the distribution of stars in the theoretical CMD for any stellar system. We compute smooth isochrones for an evolving burst population and derive by convolution the CMD of any stellar population. For a burst population, we know at any age the positions in the CMD of stars for which evolutionary tracks are available. Instead of binning stars in mass and assigning all stars in a mass bin to a given evolutionary track, we compute continuous (in mass) isochrones by interpolating between the tracks in the CMD the positions of stars of intermediate masses. The number of stars of a given mass on the isochrone is inferred from the IMF. The integrated colors and magnitudes of a burst population computed in this way vary naturally smoothly. Also, this approach is free from the approximations of models based on the fuel consumption theorem. While similar isochrone computations are commonly used to study the ages and colors of globular clusters (Becker and Mathews 1983; Chiosi, Bertelli, and Bressan 1988), we are not aware of their application to population synthesis of galaxies. We optimize our isochrone synthesis models by assembling a library of stellar evolutionary tracks based on updated stellar models in good agreement with the observations. To avoid model uncertainties, we determine semi-empirically the positions in the theoretical CMD of stars on the late AGB. The resulting tracks extend from the zero-age main sequence (ZAMS) up to the beginning of the white-dwarf cooling sequence. These tracks are for solar metallicity only. Although evolutionary tracks for other metallicities are available (e.g., Becker 1981; Chiosi *et al.* 1988; Maeder 1990), the lack of photometric calibrations for nonsolar abundances is a serious handicap to their implementation in population synthesis models.

We use our isochrone synthesis models to compute the time evolution of the bolometric and broad-band *UBVRIJKL* luminosities of a burst population. Here, and throughout this paper, a (single) burst population refers to a system in which star formation occurred instantaneously at $t = 0$. We compute the fractional contribution of each stellar evolutionary stage to the integrated light in each waveband. Furthermore, we quantify the accuracy of models based on the fuel consumption theorem by comparing their predictions with our results for the same library of tracks. Since stellar systems with any star formation rate (SFR) can be expanded in a series of burst populations, the colors of star clusters which form on rapid time scales are a natural test to confront the models with. Convolutions of the burst model with SFRs that last over longer time scales ($> 10^8$ yr) can then be used to compare the predicted colors with observed colors of present-day galaxies of various morphological types. The spectral energy distributions associated with the present photometric models of isochrone synthesis will be presented in a forthcoming paper.

In § II below we discuss how the complete set of evolutionary tracks was assembled. The details of the procedure are given in the Appendix. In § III we introduce the isochrone synthesis models and analyze the bolometric luminosity evolution of a burst population. We use our results to evaluate the accuracy of models based on the fuel consumption theorem, and compare our predictions with earlier work. In § IV we discuss the properties of several relevant isochrone synthesis models in various broad-band filters and compare our predictions with observations. Section V is a summary and conclusion to our work.

II. STELLAR EVOLUTIONARY TRACKS

In this section we put together a library of stellar evolutionary tracks whose quality relies on the following attributes: (1) the tracks include all post–main-sequence evolutionary stages. This is crucial since in particular, AGB stars are known to strongly dominate the near-IR light of star clusters at some stages of their evolution (e.g., Persson *et al.* 1983). Also, the nuclei of planetary nebulae (PNs) have been argued to cause the UV light excess observed in several elliptical galaxies (Burstein *et al.* 1988); (2) by reducing to only a few the sources of the various tracks in the library, we limit the inconsistencies introduced when assembling many stellar tracks which rely on different input physics. We also adopt among the most recent stellar models those in best agreement with the observations; (3) the luminous double-shell burning regime that low- and intermediate-mass stars undergo on the upper AGB is poorly understood by the theory. We circumvent the subjectivity of existing models

by deriving semi-empirically the locus of these stars in the theoretical CMD. In § II*a* below we summarize the approach adopted to complete points 1–3. The Appendix contains a detailed description of this procedure. In § II*b* we briefly comment on the behavior of the initial-mass/main-sequence lifetime relationship inferred from the new library of tracks.

a) Assembling of the Track Library

We first recall some nomenclature relevant to stellar evolution. Stars are usually classified according to their mass in three categories which share different properties and evolutions (Iben 1967, 1974; Iben and Renzini 1983; Chiosi and Maeder 1986). The limiting masses between categories somewhat depending on the input physics, we adopt here the recent determinations of MM.

Massive stars with masses above $\gtrsim 8\ M_\odot$ go through all nuclear burning phases until the formation of an iron core. Their subsequent fate is either a type II or Ib supernova, followed by the formation of a neutron star or a black hole. *Intermediate-mass* stars are those with initial masses in the range $M_{\rm HeF} \lesssim m \lesssim M_{\rm up}$, where $M_{\rm HeF} \approx 1.85\ M_\odot$ is the minimum mass limit for quiet He-ignition and $M_{\rm up} \approx 6.6\ M_\odot$ is roughly the maximum mass limit for degenerate C-ignition. After core-He exhaustion, intermediate-mass stars ignite helium in a shell which expands outward and causes the surrounding hydrogen shell to extinguish. This constitutes the early AGB (E-AGB) phase, since stars then undertake their second ascent of the giant branch in the CMD. Although the detail of the evolution along the AGB depends on the initial mass, all stars reignite their hydrogen shell at some point and enter the double-shell burning phase characterized by the periodic thermal pulses of the He shell. This constitutes the thermally pulsing AGB (TP-AGB) phase. Throughout this paper, the term AGB refers to the evolution from the beginning of the E-AGB until the end of the TP-AGB. Intermediate-mass stars then lose their envelope, leading to the formation of a PN and a white dwarf. The evolution of stars with masses in the range $6.6\ M_\odot \lesssim m \lesssim 8\ M_\odot$ is uncertain. They most likely undergo nondegenerate (off-center) C-ignition (MM) at the end of their E-AGB evolution, and may either become white dwarfs if they lose enough mass (Weidemann and Koester 1984) or collapse as neutron stars (Nomoto 1987). They do not go through the TP-AGB regime. Finally, *low-mass* stars with $0.08\ M_\odot \lesssim m \lesssim M_{\rm HeF}$ ignite helium degenerately (the "He-Flash") at the tip of the red giant branch (RGB), after which their evolution is similar to that of intermediate-mass stars.

Recently, MM computed a wide set of evolutionary tracks for stars with solar abundances ($Y = 0.28$ and $Z = 0.02$). The tracks extend from the ZAMS up to advanced evolutionary stages for stars with masses $1\ M_\odot \leq m \leq 120\ M_\odot$. However, several stages of late stellar evolution are missing in some tracks. The models developed by MM constitute, at the present time, the state of the art calculations of stellar evolution. They include updated values of the parameters that control stellar evolution, e.g., opacities, reaction rates, abundances, mass loss, etc. (Maeder 1989). Also, the efficiency of convective overshooting (e.g., Maeder 1976) is a very controversial problem faced by the stellar evolution theory (Renzini 1987 and references therein). MM attempted to determine this efficiency from a comparison of their models with several observable features sensitive to this parameter. To build our library of tracks, we therefore use the calculations of MM for the entire range of masses and evolutionary phases they investigated.

MM followed the evolution of massive stars up to the end of the core C-burning phase. The supernova event that terminates the life of these stars occurring only a few months or years later (Woosley and Weaver 1986), the MM tracks in this mass range do not need to be complemented. Similarly, the $7\ M_\odot$ model (the only model in the range $6.6\ M_\odot \leq m \leq 8\ M_\odot$) is followed up to the end of the E-AGB phase, presumably close to the remnant stage. The tracks of low- and intermediate-mass stars, however, do need to be largely complemented, as we now indicate.

1. MM stopped their models for low-mass stars at the helium flash. Among the various prescriptions for the subsequent evolution of these stars, none relies on the same input physics as used in MM. The recent models for various metallicities developed by Bressan, Bertelli, and Chiosi (1986) and Chiosi *et al.* (1988), however, provide the best agreement with the observations up to the end of the E-AGB phase (Appendix). We thus use evolutionary tracks computed as prescribed by Bressan *et al.* (1986) but for solar metallicity, to describe the evolution of low-mass stars through the core-He burning (CHeB) phase (the "clump" for solar metallicity) up to the end of the E-AGB (material kindly made available to us by Dr. C. Chiosi). These models favor a higher efficiency of convective overshooting than adopted by MM.

2. MM did not follow the evolution of intermediate-mass stars beyond the end of the E-AGB phase. In fact, theoretical models at this stage become very uncertain and speculative (Chiosi *et al.* 1988). Hence, for low- and intermediate-mass stars we evaluate semi-empirically the position of the TP-AGB in the theoretical CMD. Stars that pulsate on the late AGB undergo substantial mass loss and build up a circumstellar shell which re-radiates some of the star light in the infrared. The growing number of optical/infrared observations has led to the following scenario (e.g., Bedijn 1988): Mira variables have periods of a few hundred days and thin envelopes. They are interpreted as stars on the early TP-AGB. Gradually, their circumstellar shell builds up and develops OH (1612 MHz) masering. Owing to an increase of the mass-loss rate, the shell thickens, reradiates substantial amounts of star light in the infrared, and becomes a strong OH emitter. Meanwhile, the pulsation period also increases by a factor of ~ 2. Such stars have been observed as OH/IR very long period variables. They are reaching the end of their TP-AGB evolution. In the Appendix we determine the loci in the theoretical CMD of the beginning (Mira phase) and the end (OH/IR phase) of the TP-AGB, for each of the progenitor masses corresponding to the MM tracks. We use the samples of Miras and OH/IR stars analyzed by Herman *et al.* (1986) and Herman and Habing (1985). We find that the positions of the stars in the theoretical CMD (see Fig. 12 below) depend only weakly on the few necessary assumptions made on the input physics. For a given progenitor mass, we infer the durations of the lower and upper TP-AGB phases from models which reproduce acceptably well the observed statistical properties of local Miras and OH/IR variables (Bedijn 1988). The resulting TP-AGB in Figure 12 below refers to the *central* star whose appearance is then affected by the circumstellar shell.

3. At the end of the AGB, low- and intermediate-mass stars lose their envelope, leading to the formation of a PN. The central stars of PNs, or post–AGB (PAGB) stars, have fading times which strongly depend on the core mass at PN ejection

(e.g., Iben and Renzini 1983). These stars only contribute to the integrated continuum of the stellar population once the surrounding nebula had dissipated. Radio observations by Spergel, Giuliani and Knapp (1983) suggest that stars more massive than $\gtrsim 2.5\ M_\odot$ do not lead to bright PN nuclei because of their short fading time. For lower masses, the fading time is so long that the nebula can disperse before the bright PN nucleus fades. In the Appendix, we use the evolutionary tracks of Schönberner (1983) to describe the evolution of stars $\lesssim 2.5\ M_\odot$ through the bright PAGB phase.

4. MM did not compute evolutionary tracks for stars below 1 $M_\odot$. To complement our library of tracks down to lower masses, we use the 0.9 $M_\odot$, 0.8 $M_\odot$, and 0.7 $M_\odot$ models calculated by Chiosi and collaborators for solar-metallicity stars. These tracks are from the same set used in point 1 and were chosen on the same grounds as earlier. They cover from the ZAMS up to the end of the E-AGB. We complement the 0.9 $M_\odot$ model beyond the E-AGB as explained in points 2 and 3. The 0.8 and 0.7 $M_\odot$ stars have main-sequence lifetimes longer than a Hubble time.

5. Finally, we extrapolate the ZAMS down to a bolometric magnitude of ~ 11 (corresponding roughly to a mass 0.1 $M_\odot$) to include the ZAMS positions of nine (essentially unevolving) masses in the range $0.1\ M_\odot < m < 0.7\ M_\odot$. This brings up to 32 the number of tracks in the library.

b) Relationship between ZAMS Mass and Main-Sequence Lifetime

In Figure 1 we show the ZAMS mass as the function of main-sequence lifetime for the stars in the library (*solid line*). Figure 1 also indicates the ZAMS-progenitor mass of the turnoff mass as a function of the age for a burst population. The dashed line is the analytical fit of Renzini and Buzzoni (1986), who used stellar models without convective overshooting. The lengthening of the main-sequence lifetime in the new library is precisely the signature of convective overshooting (MM). Overshooting occurs in stars which develop a convective core on the main sequence. While stars below 1.1 $M_\odot$ stop developing a convective core, the efficiency of overshooting could already drop in slightly more massive stars ($\lesssim 1.5\ M_\odot$). Maeder (1989) comments on the difficulties encountered by the theory in the treatment of the transition region $1.1\ M_\odot \lesssim m \lesssim 1.5\ M_\odot$. He complements the tracks computed by MM in this region by a set of models without overshooting. In the absence of any convincing evidence in favor of the latter, we use the tracks with overshooting down to 1.15 $M_\odot$. For lower masses then (lifetimes $\gtrsim 10$ Gyr), the relation used by Renzini and Buzzoni (1986) matches that of the new library.

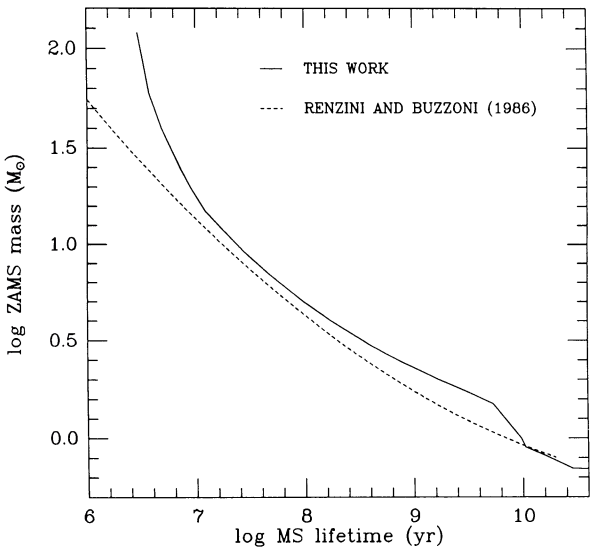

FIG. 1.—ZAMS mass as a function of main-sequence lifetime for stars in the library of evolutionary tracks assembled in § II*a* (*solid line*). The dashed line is the analytical fit of Renzini and Buzzoni (1986) who used models without overshooting. This figure also indicates the ZAMS–progenitor mass of the turn-off mass as the function of the age for a burst population.

III. ISOCHRONE SYNTHESIS MODELS

We consider here a method of population synthesis that allows us to compute the distribution of stars in the theoretical CMD more accurately than conventional models of population synthesis or models based on the fuel consumption theorem. Since any stellar system can be expanded in a series of burst populations, it is indicated to compare the various methods of population synthesis on the basis of their computations of isochrones for burst populations. In conventional population synthesis, stars are binned in mass so that all stars in a given mass bin evolve on a single evolutinary track. At a given age, stars in one bin populate a segment on their track whose length is determined by the star age dispersion and in turn by the star formation time scale. For a burst stellar population, all stars have the same age, and each segment is reduced to a single evolutionary stage on the tracks. Thus, an isochrone is defined by a number of points in the theoretical CMD equal to the number of tracks in the library. The computed colors and magnitudes change then abruptly as stars in a given mass bin suddenly "jump" into a different evolutionary stage. For instance, the optical/near-IR colors of a burst population may drop instantaneously by more than 1 mag (depending on the resolution in mass of the stellar tracks library) as evolved stars in a given mass bin reach the end of their track (luminous red) and then die. Due to the finite number of tracks, stars in the consecutive mass bin reach the end of their track (and produce another red flash) at later ages only. Hence, for conventional population synthesis to model smoothly the evolution of a burst population, a continuous (in mass) set of evolutionary tracks would be needed. Population synthesis models based on the fuel consumption theorem do not either provide us with a mean to distribute stars accurately in the theoretical CMD. The fuel consumption theorem (see § I) expresses the proportionality between the amount of nuclear fuel burned by stars during their post–main-sequence evolution and their contribution to the integrated bolometric light of the stellar population. However, when used in models of population synthesis, this theorem is generally coupled with several simplifying assumptions. Indeed, for a burst stellar population, such models approximate an isochrone beyond the main sequence by the evolutionary track of the turn-off mass and assign the same IMF weight to all evolved stars. This may introduce some errors in the photometric properties of the stellar population which have never been evaluated properly.

We now consider an alternative approach to population synthesis. For a burst population, we know at any time the positions in the theoretical CMD of stars for which evolutionary tracks are available. Instead of binning stars in mass and assigning each mass bin to a given evolutionary track, we

compute continuous (in mass) isochrones by interpolating between the tracks in the theoretical CMD the positions of stars of intermediate masses. This requires to identify stages of equivalent physical significance in the available tracks corresponding to different masses (Maeder and Meynet 1988). Indeed at a given age, stars on two consecutive tracks populate two stage of different physical significance. One must assign consistent evolutionary stages to stars whose positions are interpolated between those two tracks. For this purpose, a total of 155 stages of distinct physical significance were identified in the stellar evolutionary tracks. Isochrones computed in this way define at each age a continuous sequence in mass from the lower mass limit of the IMF up to the mass of dying stars. Each mass occupies its exact position in the theoretical CMD and is not rigidly assigned to a particular track. Also, the integrated colors and magnitudes of the burst population vary smoothly in time since continuity is guaranteed in the distribution of stars from the main sequence, through the turnoff, up to dying stars (at a given time, the positions in the CMD of stars in these stages may or may not coincide with positions on the original tracks). The number of stars of a given mass on the isochrone is inferred from the IMF. In studies of star clusters (in which isochrones are currently computed in this way), Monte Carlo simulations are used at this point to mimic the stochastic effects caused by the small number of stars (Chiosi *et al.* 1988 and references therein). For larger systems it is more appropriate to use nonprobabilistic techniques. From the number of stars at each position in the theoretical CMD, one can then compute the observable properties of a burst stellar population. In the limit of constant metallicity and IMF, we can infer by a simple convolution the properties of stellar systems with arbitrary SFRs. Hence, unlike conventional models of population synthesis, the present approach does not require *a posteriori* smoothing of the integrated properties of stellar populations forming on short time scales. The isochrones are first interpolated and the integrated properties are then evaluated, by means of a convolution.

Although very simple conceptually, the isochrone synthesis approach requires a complete library of evolutionary tracks for which physically equivalent stages can be identified. This may be one reason why this technique has not been used before in population synthesis models of galaxies. We note that in practice, conventional models of population synthesis would be equivalent to our isochrone synthesis models if a continuous (in mass) set of stellar evolutionary tracks were available. In the following, we first analyze the evolution of the bolometric luminosity of an evolving burst population with particular attention to the AGB contribution. By computing with the same library of tracks the evolution of the bolometric luminosity as prescribed by models based on the fuel consumption theorem, we can determine properly their accuracy. We then briefly compare our results with previous predictions.

a) Evolution of the Bolometric Luminosity of a Burst Population

In Figure 2 we show the evolution of the integrated bolometric luminosity of a burst population (*solid line*) in which stars were distributed according to the Salpeter (1955) IMF. The integrated luminosity decreases smoothly from early times until ~ 10 Gyr, as the turnoff mass lowers. The relative increase of the luminosity afterward deserves comment. It is due to the conspiracy of three effects. First, the age range 8–10 Gyr marks the transition between stellar models with and without convective cores. Stars with no convective cores spend more time burning fuel off the main sequence, at higher luminosities. Second, both the luminosity extension and lifetime of the RGB phase increase with decreasing ZAMS mass for low-mass stars. Third, because of the slope of the IMF, lower mass stars which spend more time at higher luminosities are also more numerous.

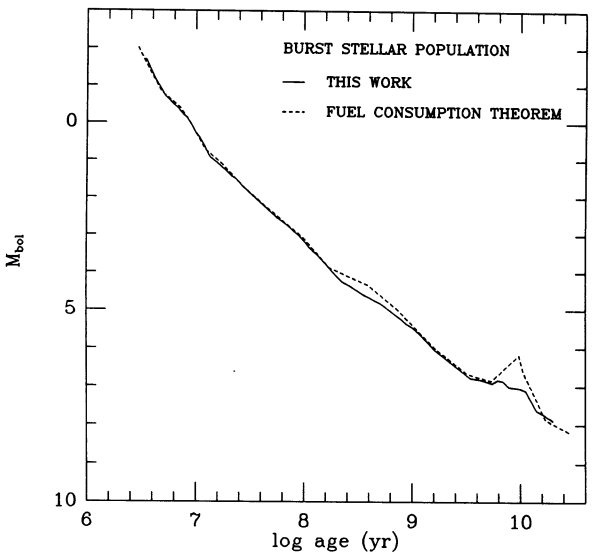

FIG. 2.—Evolution of the integrated bolometric magnitude of a burst population. The solid line is the prediction of the isochrone synthesis model. The dashed line was computed by applying the fuel consumption theorem to the same library of tracks. The stellar population in both cases has a total mass of 1 $M_\odot$ distributed according to the Salpeter (1955) IMF.

It is instructive to analyze the contribution of the main sequence and various post–main-sequence evolutionary stages to the integrated bolometric luminosity, as shown in Figure 3*a*. We have combined the 155 stages of distinct physical significance identified earlier into 6 broad classes (main sequence, SGB, RGB, CHeB, AGB, and PAGB). The fluctuations seen in some of the curves are intrinsic to the stellar tracks, since the contribution of a given evolutionary phase does not always vary smoothly with decreasing ZAMS mass. A striking feature is that main-sequence stars dominate the integrated light of the burst population from early ages on until ~ 8 Gyr, contradicting ealier predictions (Renzini and Buzzoni 1986). This predominance is essentially due to the inclusion of convective overshooting in MM stellar tracks, that lengthens the main-sequence lifetime of stars more massive than 1.1 $M_\odot$. Since lower mass stars do not develop a convective core on the main sequence, RGB stars dominate the bolometric light at later ages. In particular, from 1 to 8 Gyr the contribution of post–main-sequence stages never exceeds 25%, whereas after 9 Gyr the RGB accounts for $\sim 50\%$ of the light.

The results shown in Figure 3*a* can be summarized as follows. At early ages, 60%–75% of the light is accounted for by main-sequence stars (of spectral types O through B5) while core-He burning stars provide the remaining 25%–40%. When the AGB turns on (around 0.1 Gyr), the main sequence and CHeB contributions start decreasing noticeably. At the maximum of their contribution (0.4–1.6 Gyr), AGB stars account for 35% of the light. At this time the main sequence (spectral types B5–A7) still dominates with a 45% contribution while CHeB stars provide the residual 20%. The next few billion years (1.5–8 Gyr) are marked by a strong leadership of main-sequence stars (of spectral types A7–G0) which contrib-

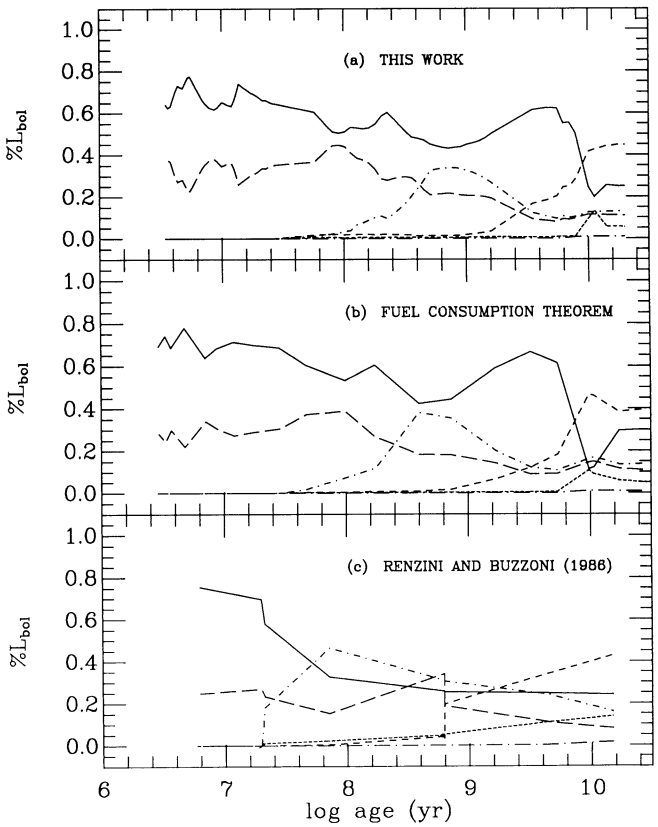

FIG. 3.—Fractional contribution of the various stellar evolutionary stages to the integrated bolometric luminosity of a burst population as a function of time (IMF from Salpeter 1955). The three panels correspond to (*a*) the isochrone synthesis model; (*b*) the fuel consumption theorem applied to the same library of tracks as in (*a*); (*c*) the results obtained by Renzini and Buzzoni (1986) by applying the fuel consumption theorem to their own library of tracks. In all panels the different curves correspond to the following stellar evolutionary stages: main sequence (*solid line*), SGB (*short-dashed line*), RGB (*dashed line*), CHeB (*long-dashed line*), AGB (*dot and short-dashed line*) and PAGB (*dot and long-dashed line*).

ute ~60% of the light. Meanwhile, the AGB and CHeB stars both drop to a 10% contribution and the RGB develops (providing ~20% of the light) due to the appearance of stars with degenerate He cores. After 9 Gyr the RGB (~50%) imposes on the main sequence (~20%–25%) while AGB and CHeB stars stabilize around ~10%. Furthermore, since stars do not develop a convective core any more on the main sequence, the SGB phase is lengthened and provides ~5%–10% of the light. Stars on the PAGB hardly contribute to the integrated light even at very late ages.

Figure 4 illustrates in more detail the behavior of AGB stars in our models. The data in Figure 4*a* represent the fractional bolometric luminosity of Magellanic Clouds clusters of various ages accounted for by AGB stars brighter than $M_{bol} \lesssim -3.6$ (from Frogel *et al.* 1990). The solid line is the fractional contribution of stars brighter than this limit as predicted by our models for a burst population (the burst model is suited to the study of clusters which form on time scales $\lesssim 10$ million yr). The general agreement of model with data is very good, especially since the youngest clusters may be contaminated by M supergiants mistaken for AGB stars (Frogel *et al.* 1990). In Figure 4*b* we show the total AGB contribution (*dashed line*), the contribution of AGB stars brighter than $M_{bol} \lesssim -3.6$ (*solid line*, from Fig. 4*a*) and the contribution of the empirically derived TP-AGB (*dot-dashed line*) to the bolometric light of a burst model. TP-AGB stars account for 45% of the total AGB luminosity around 0.1 Gyr. After 1 Gyr they contribute only 15% of the AGB light. The fraction of the integrated bolometric light of the stellar system accounted for by TP-AGB stars never exceeds 10% (though these stars may produce ≈20% of the near-IR light at some stages, see § IV).

b) Accuracy of Models Based on the Fuel Consumption Theorem

We now compute the evolution of the bolometric light of a burst population as prescribed by models based on the fuel consumption theorem. The fuel consumption theorem expresses rigorously the proportionality between the bolometric light of a stellar population accounted for by evolved stars in a given evolutionary stage and the amount of nuclear fuel burned by these stars. However, this theorem is generally coupled with several simplifying assumptions when used in

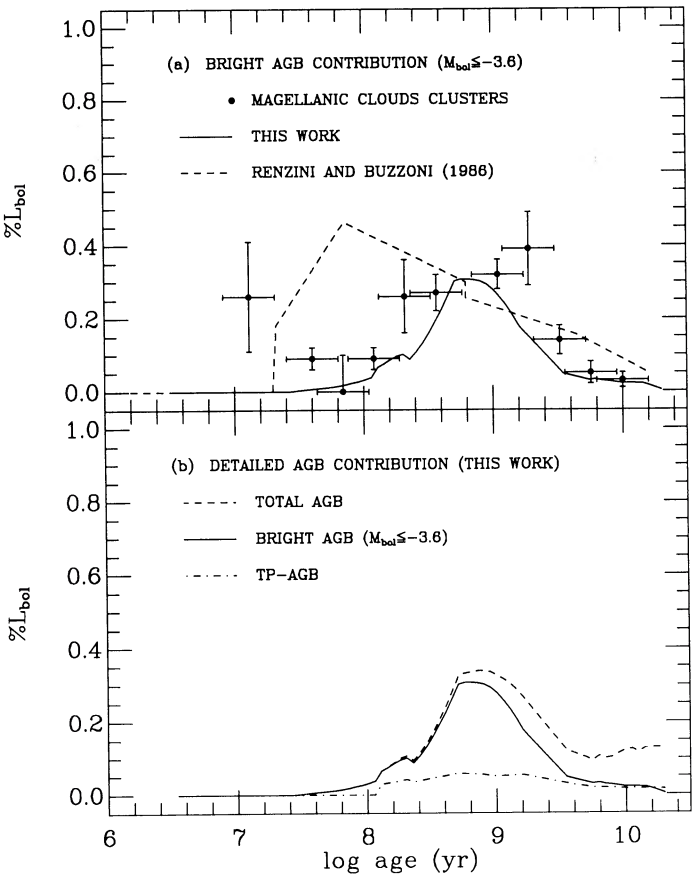

FIG. 4.—(*a*) Fractional contribution of bright AGB stars ($M_{bol} \lesssim -3.6$ mag) to the integrated bolometric light of a burst population. The solid line is the contribution predicted by the isochrone synthesis model. The data are the contribution observed in the Magellanic Clouds star clusters by Frogel *et al.* (1990). A mean cluster age uncertainty of ≈0.2 in log was estimated from their paper. The apparent rise of the AGB contribution in the youngest clusters may result from contamination by red supergiants in the data. The dashed line is the contribution predicted by Renzini and Buzzoni (1986), corrected as indicated in Frogel *et al.* (1990) to account for the truncation of the observed AGB below $M_{bol} \gtrsim -3.6$. (*b*) Fraction of the integrated bolometric light of a burst population accounted for by all AGB stars (*dashed line*), bright ($M_{bol} \lesssim -3.6$) AGB stars (*solid line*) and TP-AGB stars (*dot-dashed line*), as predicted by the isochrone synthesis model.

models of population synthesis. For a burst population, such models approximate at a given age the IMF–weighted isochrone beyond the main sequence by the evolutionary track of the turnoff mass. All stars on this track are assigned the IMF weight of the turnoff mass. To perform a meaningful comparison with our isochrone synthesis models, we must compute fuel consumption theorem models using the new library of tracks. Differences in the results obtained with the two approaches will then reveal the intrinsic limitations of models based on the fuel consumption theorem. More precisely, such a comparison allows us to quantify the approximation of replacing an interpolated, IMF–weighted isochrone (isochrone synthesis model) beyond the main sequence by the evolutionary track of the turnoff mass with uniform IMF weight (the intrinsic assumption of models based on the fuel consumption theorem). This approximation, and in turn the inferred limitations of models based on the fuel consumption theorem, are independent of the choice of the stellar tracks library. We take the latter to be the same in both models for comparison purposes. The evolution of the bolometric luminosity calculated in this way is shown in Figure. 2 (*dashed line*) for a Salpeter IMF. We have computed the "evolutionary flux" of post–main-sequence stars, $b(t) = \phi(M_{\rm TO})|dM_{\rm TO}/dt|$ (Renzini 1981), by estimating numerically $dM_{\rm TO}/dt$ at each time step (Fig. 1). In this expression, $M_{\rm TO}$ is the turnoff mass at age t and $\phi(M_{\rm TO})$ parametrizes the IMF. Although the predictions of the fuel consumption theorem model and the isochrone synthesis model shown in Figure 2 are very close, one can identify two small but significant differences.

1. The fuel consumption theorem model predicts in average slightly higher luminosities than our isochrone synthesis model. Indeed, evolved stars have, in general, smaller IMF weights and shorter lifetimes than the stars at the turnoff. By assigning the same IMF weight and post–main-sequence lifetime to all stars above the turnoff, the fuel consumption theorem model *overestimates* the contribution of luminous evolved stars to the integrated light of the population. This effect is particularly apparent around 10 Gyr when the post–main-sequence lifetime of stars increases sharply.

2. On the other hand, the luminosity reached by a star during its post–main-sequence evolution is a decreasing function of ZAMS mass (at least for stars initially more massive than $M_{\rm HeF}$). Thus, the fuel consumption theorem model *underestimates* the luminosity of evolved stars by assigning them to the evolutionary track of the turnoff mass. This is particularly significant at early ages when $dM_{\rm TO}/dt$ is very high.

The end result is that the model based on the fuel consumption theorem slightly underestimates the bolometric luminosity at early ages. At later ages the effect described in point 1 prevails. After $\gtrsim$15 Gyr, the scatter in the $M_{\rm TO}$–time relationship and the small number of available tracks make numerical estimates of the evolutionary flux more uncertain. This causes the fuel consumption theorem model to appear fainter than the isochrone synthesis model.

We plot in Figure 3*b* the contributions of the various stellar groups to the integrated bolometric light of a burst model (Salpeter IMF) as prescribed by the fuel consumption theorem. Some differences with Figure 3*a* naturally follow from points 1 and 2 discussed above. In particular, the curves in Figure 3*b* appear similar to those in Figure 3*a* only "shifted" toward slightly younger ages. This is because the fuel consumption theorem model distributes post–main-sequence stars along the track of the turnoff mass, whereas this one should only populate its track at later ages. The curve corresponding to the main sequence contribution is in turn also shifted toward younger ages. Typically the shift in age in Figure 3*b* is ~20%–40% of the age determined from our more accurate isochrone synthesis model. This estimate holds for ages $\lesssim$10 Gyr, before the sparsity of the tracks affects the determination of the evolutionary flux. We note that the fuel consumption theorem model also predicts a slightly brighter peak contribution of AGB stars since it overestimates their IMF weight (point 1). This effect is less apparent for the SGB or RGB because of the smaller difference between the mass at the turnoff and the mass at those stages.

Despite the small differences outlined above, we conclude from our comparison that models based on the fuel consumption theorem are, indeed, a reasonable approximation to study the evolution of the bolometric luminosity of star systems. The main disadvantage of such models is that they somewhat underestimate the age of a burst population derived from a given distribution of the light among the various stellar evolutionary stages. Again, the limitations identified above of models based on the fuel consumption theorem are entirely due to their intrinsic assumption that at a given age, the IMF-weighted isochrone beyond the main sequence can be replaced by the evolutionary track of the turnoff mass. These conclusions do not depend on the choice of the stellar tracks library. We emphasize that although the fuel consumption theorem has already been used in several studies (Renzini and Buzzoni 1986; Buzzoni 1990), this is the first time the accuracy of models based on this theorem is evaluated.

c) *Comparison with Previous Work*

Regardless of the way the distribution of stars in the theoretical CMD is computed, the new library of stellar tracks used in this work leads to important revisions of previous results obtained with population synthesis models. We show in Figure 3*c* the predictions of Renzini and Buzzoni (1986) for the fractional contribution of the various stellar stages to the integrated light of a burst population (Salpeter IMF). They computed these results using the fuel consumption theorem but with different stellar models. The discrepancies between Figures 3*b* and 3*c* are therefore a consequence of updating the stellar tracks. In particular, Renzini and Buzzoni largely overestimated the contribution of AGB stars (Fig. 4*a*). Also, they did not take convective overshooting into account in their models so that they underestimated the main-sequence lifetime of stars more massive than ~1.1 $M_\odot$. We note that Renzini and Buzzoni's results roughly agree with our predictions at very late ages. This is because low-mass stars do not suffer convective overshooting, and the difference in the stellar models is less significant.

The use of an accurate library of stellar tracks has therefore crucial implications on the results provided by population synthesis models, regardless of the computational method adopted. In this sense, the present work is an improvement over existing models which use a less updated stellar input physics. Bruzual (1983) uses stellar tracks which do not include the late stages of stellar evolution (e.g., CHeB and AGB). Guiderdoni and Rocca-Volmerange (1987) and Buzzoni (1990) adopt the same prescription as Renzini and Buzzoni (1986) to describe the evolution of stars on the AGB.

IV. APPLICATION TO THE PHOTOMETRIC EVOLUTION OF STELLAR SYSTEMS

In this section, we use our isochrone synthesis models to compute the photometric evolution of stellar populations with

various SFRs and IMFs. This requires knowledge of the photometric properties of stars at any given position in the theoretical CMD. Using standard calibrations (Flower 1977; Böhm-Vitense 1972), we transform the stellar evolutionary tracks in the theoretical CMD (§ II) into tracks in the observational (V, $B-V$) CMD. Using Johnson (1966) calibration of the *UBVRIJKL* photometric system (luminosity classes I, III, and V) we then compute the associated $U-B$, $V-R$, $V-I$, $V-J$, $V-K$, and $V-L$ colors at each position on the tracks. Stars hotter than log $T_{\rm eff} \approx 4.7$ are not included in the calibration relationships due mainly to their scarcity. We therefore derive the colors of these stars from the spectral energy distribution of a blackbody of same temperature. The colors of stars on the TP-AGB must take into account the reddening by their circumstellar shell. For each evolutionary track of low- and intermediate-mass star, we have defined in § II*a* and calculated in the Appendix the luminosities, central star temperatures, and durations of the lower TP-AGB (Mira phase) and upper TP-AGB (OH/IR phase). Due to the small dispersion in effective temperatures for stars of various masses on their TP-AGBs (Fig. 12 below), we assume that all stars on their lower TP-AGB have the colors of Mira Ceti and all stars on their upper TP-AGB have the colors of IK Tau (the luminosities and times spent in the two phases remaining proper to each evolutionary track). These two stars have colors representative of observed Miras and OH/IR stars (e.g., Reid, Tinney, and Mould 1990). Their bolometric corrections were derived by combining the data of Zhou *et al.* (1986), Dyck *et al.* (1974), and Herman *et al.* (1986). Once the photometric properties of all stars in the library are known, we can transform isochrones in the theoretical CMD into isochrones in the observational CMD for an evolving burst population. The photometric properties of populations with arbitrary SFRs are then inferred by a simple convolution. More precisely, let $w_0(\tau)$ be the number of stars at a given position in the CMD for a burst population of age τ. In a stellar system with arbitrary SFR $\Psi(t)$, the number $W_0(t)$ of stars at this position at age t is given by the convolution integral

$$W_0(t) = \int_0^t \Psi(t-\tau) w_0(\tau) d\tau \ . \qquad (1)$$

The flux emitted by these stars at wavelength λ is $W_0(t)F_0(\lambda)$, where $F_0(\lambda)$ is the flux emitted by one star at this position.

In the following, we investigate the evolution of the *UBVRK* integrated magnitudes and colors of several isochrone synthesis models and compare our results with earlier predictions. In all models the IMF extends from $m_L = 0.1\ M_\odot$ up to $m_U = 125\ M_\odot$. We then analyze the contributions of the various stellar evolutionary stages to the *UBVRIJKL* luminosities. Finally, we compare our predictions with the observed colors of star clusters and bright galaxies.

a) Magnitudes and Colors versus Age

In Figure 5 we show the evolution of the bolometric and *UBVRK* magnitudes of three models with different SFRs and the Salpeter IMF. The behavior of some representative colors is shown in Figure 6. The SFR is normalized in such a way that 1 solar mass of gas is transformed into stars over the life of the system. As star formation progresses the luminosity rises in all bands. When star formation ceases in the models, the luminosity drops in all bands because of the disappearance of bright main-sequence and supergiant (CHeB) stars. The red supergiants induce a bump in the K luminosity of the burst model

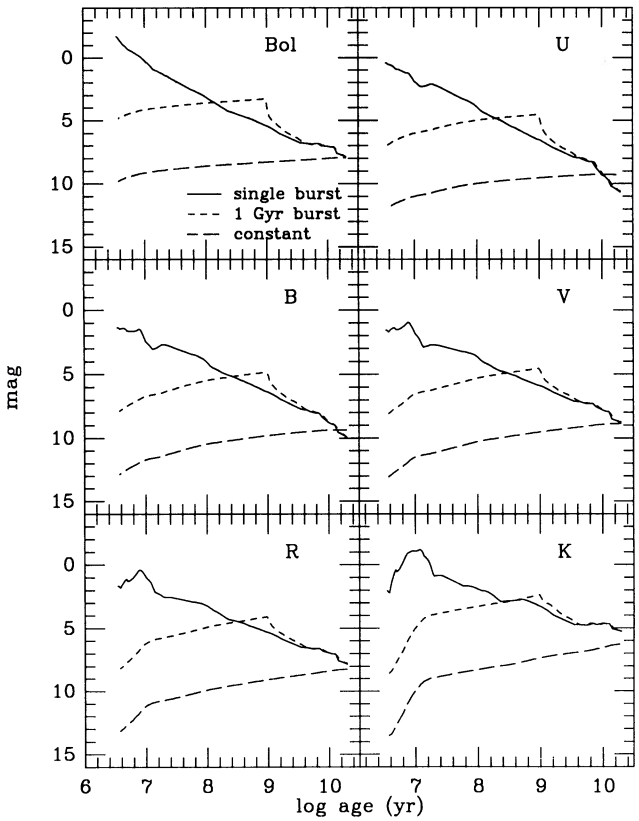

FIG. 5.—Evolution of the integrated bolometric and *UBVRK* luminosities of isochrone synthesis models with different SFRs. The SFRs in the three models shown are: single burst (*solid line*), 1 Gyr burst (*short-dashed line*); constant (*long-dashed line*). In all models the IMF is from Salpeter (1955).

around 1×10^7 yr. It is likely that this "excursion in the red" (Fig. 6) corresponds to that identified by Bica, Alloin, and Santos (1990) in the integrated light of young star clusters in the LMC. The small increase of the U, B, and V luminosities in the burst model around 2×10^7 yr is due to stars of slightly lower mass ($\lesssim 13\ M_\odot$) which burn He in their core at high temperatures and high luminosities. For models with longer time scales of star formation, these rapid excursions in the red and in the blue are smoothed away by the convolution (Fig. 6). The AGB produces an increase of the K luminosity around 0.4–2 Gyr in the single burst and the 1 Gyr burst models. This appears more clearly in the reddening of the $V-K$ color in Figure 6*c*. The evolution of the bolometric luminosity (Fig. 5) is very close to that of the V luminosity in all cases, except that the red supergiants do not produce a noticeable feature in the burst model. We note in Figure 6 that, as expected, the 1 Gyr burst model has the colors of a constant SFR model until 1 Gyr, after which it resembles closely a single burst population. The colors of an old stellar population are insensitive to the detail of its past SFR once star formation has ceased for several billion years.

In Figure 7*a*, the importance of the choice of stellar evolutionary tracks is illustrated with the $B-V$ color of the 1 Gyr burst model. Bruzual's (1983) prediction is more than 0.2 mag bluer than our isochrone synthesis model at ages $\lesssim 1$ Gyr. His model lacks the reddening caused by the red supergiants (the lack of AGB stars is less apparent in the $B-V$ color). Wyse (1985) used the prescriptions of Renzini (1981) in order to complement the Bruzual model for the lack of AGB

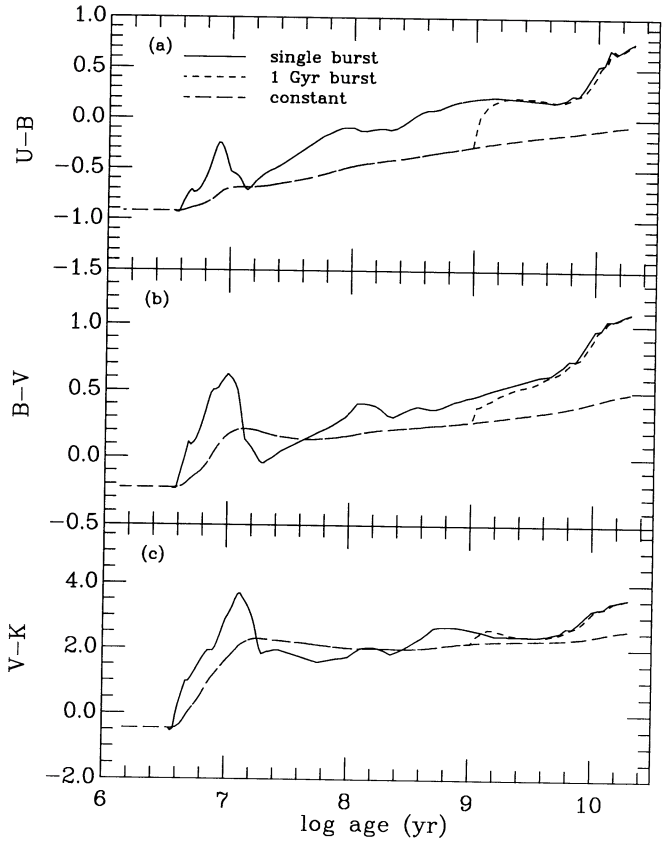

FIG. 6.—Evolution of the (*a*) $U-B$, (*b*) $B-V$, and (*c*) $V-K$ colors of the isochrone synthesis models of Fig. 5.

stars. The inferred $B-V$ color reddens too early since the AGB turns on too early and is also too bright in Renzini's prescriptions (Fig. 4*a*). Figure 7*b* illustrates the improvement of the isochrone synthesis approach over conventional population synthesis for the $V-K$ color evolution of a stellar system forming on short (1×10^8 yr) time scale. The Bruzual (1983) model shows an indented color evolution with red maxima corresponding to stars reaching the end of their track, followed by sudden transitions in the blue after they die (note also the lack of reddening due to the missing AGB around 1 Gyr). The isochrone synthesis model contrasts with a smooth evolution of the $V-K$ color.

b) Contribution of Different Stellar Groups

The integrated spectrum of a population in a given waveband resembles that of stars which dominate the emission in this waveband. We now analyze in more detail the role of each stellar group in the photometric evolution of stellar systems forming at different rates. We consider the two representative cases of a burst and a constant SFR, both computed with the Salpeter IMF. In Figures 8 and 9 we show for the two models the evolving contributions of the various stellar groups to the integrated light in the *UBVRIJKL* wavebands. Contributions to the bolometric luminosity are also indicated for reference. Again, the fluctuations in the various distributions are intrinsic to the stellar evolutionary tracks. Figure 8 shows that main-sequence stars dominate the U light of a burst population from early times up to 10 Gyr. At ages $\lesssim 0.4$ Gyr, CHeB stars compete with main-sequence stars in the emission at longer wavelengths, producing nearly the entire light from the red to the near-IR. Around 0.4–2 Gyr, the contribution of AGB stars varies from 0% in the U gradually to 70% in the L, with 5%–20% of the light from I to L produced by TP-AGB stars alone. Main-sequence stars at these ages account for most of the remaining light from U to L. From 2 to ~ 10 Gyr the main sequence then dominates the luminosity in all wavebands. After 10 Gyr the RGB takes over at wavelengths redder than R with a 40%–50% contribution. At shorter wavelengths the main sequence still dominates, followed by the RGB, AGB, and SGB. We note that PAGB stars account for only 4% of the U light after 13 Gyr, corresponding to a fractional bolometric luminosity $\lesssim 1\%$. These stars thus seem insufficent to explain the strong UV excess seen in several ellipical galaxies, at least for solar metallicity models (see Greggio and Renzini 1990 for an extensive discussion). Figure 9 shows that for constant star formation, the main sequence dominates the integrated U and B light at all ages. CHeB stars account for most of the red to near-IR luminosity over the system's lifetime. After ~ 1 Gyr, AGB stars contribute significantly (30%–40%) in the near-IR but they never dominate strikingly. At ages $\gtrsim 10$ Gyr, RGB, AGB, CHeB and main-sequence stars produce nearly the same amount of near-IR light.

Figures 8 and 9 illustrate the importance of analyzing the contributions of the various stellar groups to the integrated light in *different* wavebands. An analysis of the bolometric luminosity alone does not provide information on what features to expect in the integrated spectrum at separate wavebands, especially in the R to near-IR. We have computed

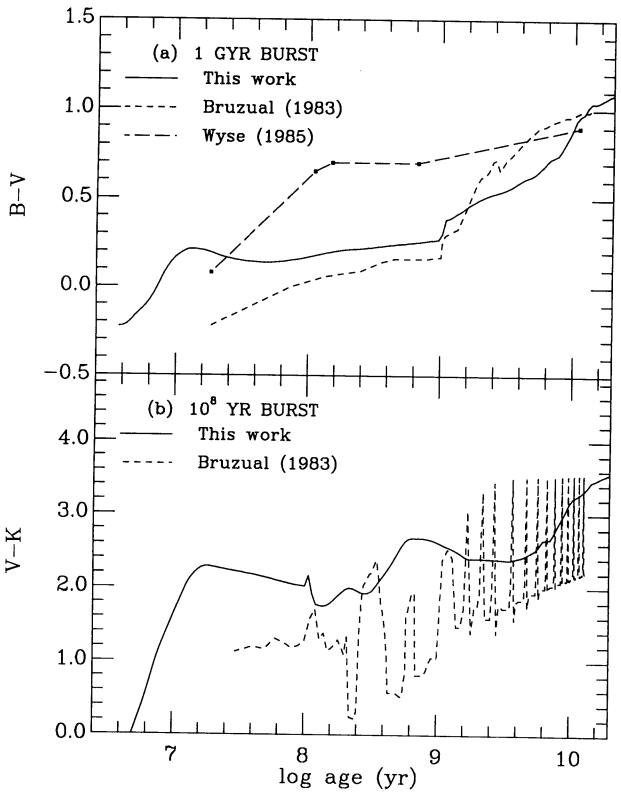

FIG. 7.—(*a*) $B-V$ color of a 1 Gyr burst population as predicted by population synthesis models computed with different stellar tracks libraries: the isochrone synthesis model (*solid line*), the Bruzual (1983) model (*short-dashed line*), and Wyse (1985, *long-dashed line*) who followed the prescriptions of Renzini (1981). (*b*) $V-K$ color of a 1×10^8 yr burst population as computed with the isochrone synthesis model (*solid line*) and the conventional population synthesis model of Bruzual (1983, *dashed line*).

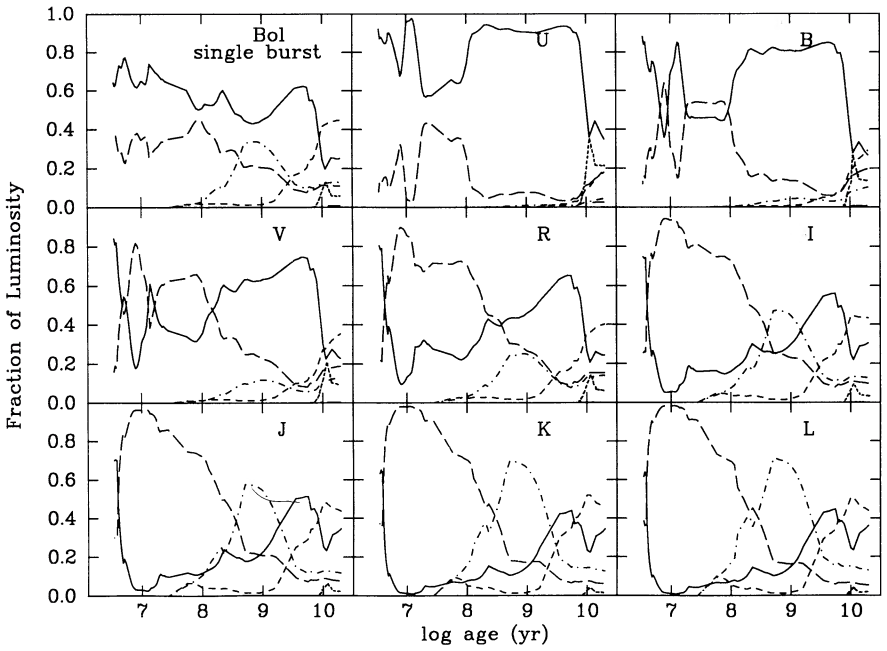

FIG. 8

FIG. 8.—Fractional contribution of the various stellar evolutionary stages to the integrated bolometric and *UBVRIJKL* luminosities of a burst population as a function of its age (IMF from Salpeter 1955). The line codes are the same as in Fig. 3.

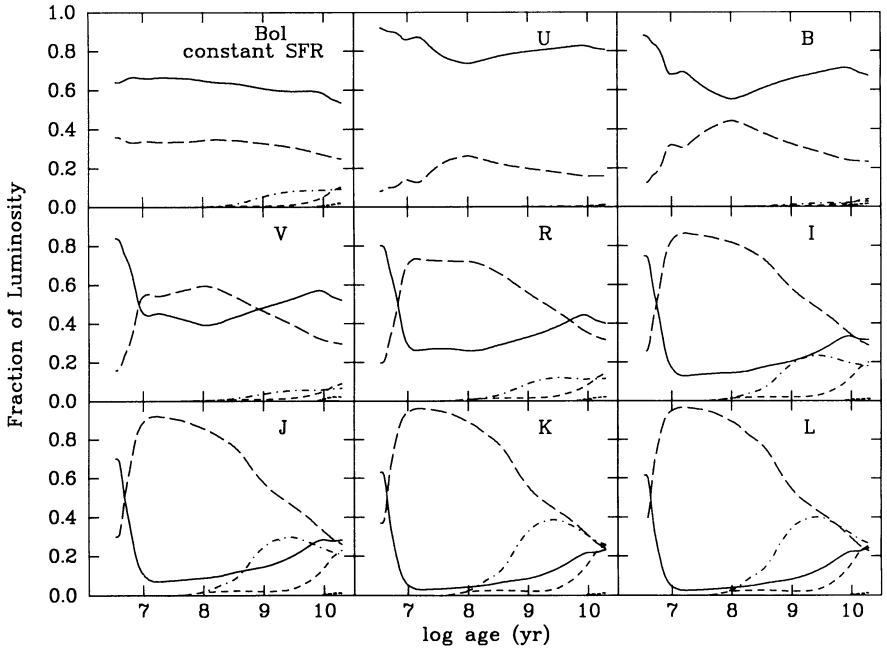

FIG. 9

FIG. 9.—Same as Fig. 8 but for a constant SFR

diagrams similar to those in Figures 8 and 9 for stellar populations with intermediate time scales of star formation. They give distributions intermediate between the two figures. Also, the results obtained by using a Scalo (1986) IMF are similar to the ones shown here.

c) *Star Cluster and Galaxy Colors*

We now compare the predictions of our isochrone synthesis models with the colors of observed stellar populations. Since a stellar system of any SFR can be expanded in a series of burst populations, the colors of star clusters which form on rapid time scales are a natural test to confront the models with. Star clusters in the LMC have ages between a few million years and a few billion years (Searle, Wilkinson, and Bagnuolo 1980; Elson and Fall 1985, 1988). They can be regarded as a collection of snap-shots of an aging stellar system which formed in a burst of duration $\lesssim 1 \times 10^7$ yr. Clusters younger than $\lesssim 2$–4 Gyr should have abundances nearly solar but older clusters are probably metal deficient (Cohen 1982). In Figure 10 we show the evolution of the $U-B$, $B-V$, and $V-K$ colors of a model stellar population (Salpeter IMF) formed in a burst of duration 1×10^7 yr (*solid line*). The data points are the colors of a representative sample of LMC clusters from Persson *et al.* (1983) with ages from Elson and Fall (1985, 1988). Given the high sensitivity of the $U-B$ and $V-K$ colors to the detail of the stellar population synthesis, the good agreement between the predicted and observed colors in Figure 10 is a strong argument in favor of the quality of the present model. In particular, the variation trend of all colors as a function of time is quite well reproduced by the model (within the observational uncertainties) until ~ 4 Gyr. As expected, our model for solar abundances cannot fit the blue colors of the older, metal-poor clusters. The ages of several of these old clusters may also have been overestimated since they were determined from a photometric age indicator in the "hook" region of the *UBV* two-color diagram (Elson and Fall 1988).

To then check the reliability of the isochrone synthesis models at later ages, we compare the predicted colors with observed colors of present-day galaxies. Since nearby galaxies of different Hubble types seem to have experienced different star formation histories (Kennicutt 1983), we investigate the photometric properties of models with various star formation laws

$$\Psi(t) \propto \exp(-t/\tau), \qquad (2)$$

where τ is the time scale of star formation. Figure 11 shows the evolution in the *UVK* two-color diagram of models with $\tau = 0.5$, 1, 2, 3, 6, and 9 Gyr and ∞ (constant SFR), all computed with the Salpeter IMF (*thick lines*). The models start in the blue region of the *UVK* plane (*upper left*) and evolve redward. The dashed lines are the locations at fixed ages (1, 5, 10, and 15 Gyr) in the *UVK* plane of models with $0.5 \text{ Gyr} \lesssim \tau \lesssim \infty$. We also indicate the mean observed colors of bright galaxies of various morphological types (from E to Im) and their dispersions (from Aaronson 1978). Figure 11 shows that all models follow a similar path in the *UVK* plane until about $\lesssim 1$ Gyr. Around this age, *all* models fit the colors of average Im galaxy. In fact, Im galaxies are known to have experienced substantial star formation in their recent past (Kennicutt 1983; Gallagher *et al.* 1984). The evolution of the

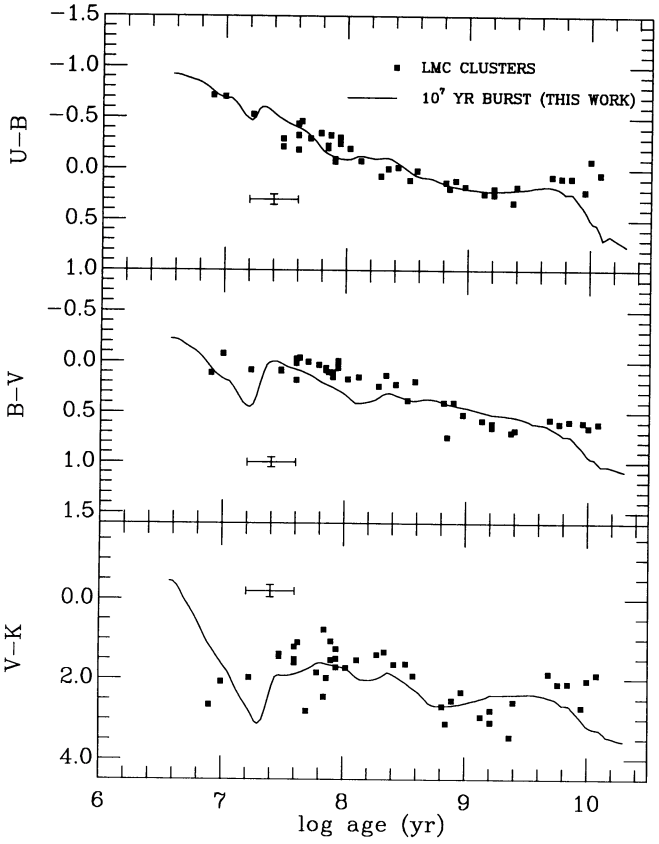

FIG. 10.—Evolution of the $U-B$, $B-V$ and $V-K$ colors of a 10^7 yr burst population computed with the Salpeter (1955) IMF (*solid lines*). The data points are from a representative sample of LMC clusters with infrared photometry from Persson *et al.* (1983) and *UBV* photometry from van den Bergh (1981). The clusters ages are from Elson and Fall (1985, 1988). All observed colors have been dereddened by using the color excesses tabulated by Persson *et al.* (1983). Typical error bars are indicated on the figures. The oldest, blue clusters in the sample are biased toward low metallicities (Cohen 1982).

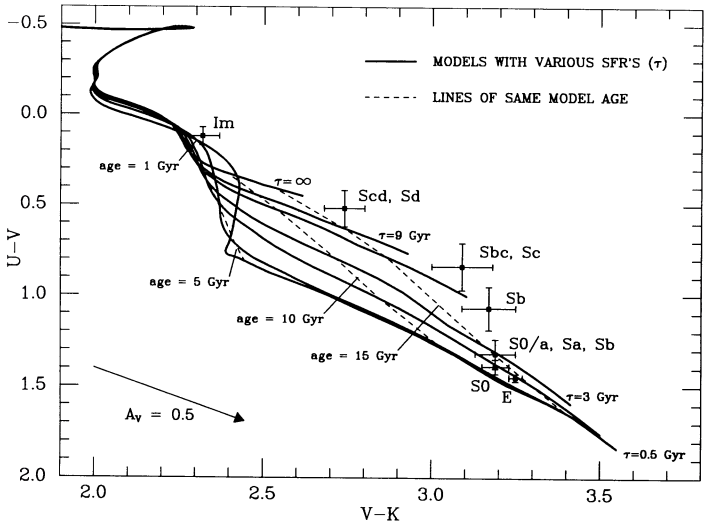

FIG. 11.—*UVK* two-color diagram of isochrone synthesis models with decaying SFRs (eq. [2]) of time scales $\tau = 0.5$, 1, 2, 3, 6, and 9 Gyr and ∞ (*thick lines*). For clarity only the curves corresponding to $\tau = 0.5$, 3, and 9 Gyr and ∞ have been labeled. The mean observed colors of bright galaxies of various morphological types (from E to Im) are indicated with their dispersions (from Aaronson 1978). The dashed lines are the locations at fixed ages (1, 5, 10, and 15 Gyr) in the *UVK* plane of models with 0.5 Gyr $\lesssim \tau \lesssim \infty$. The reddening vector is adapted from Aaronson (1978).

models thereafter depends on the shape of the SFR. Longer time scales of star formation evolve into later-type Spirals whereas rapid star-forming systems lead to early-type S0's or E's. This result is consistent with the dependence of the star formation history on morphological type inferred in an independent way from spectrophotometric observations of nearby galaxies (Kennicutt 1983; Gallagher, Hunter, and Tutukov 1984). Figure 11 brings two other interesting remarks. First, the whole possible range of star formation time scales (from burst to constant) leads precisely to the observed UVK color range of all morphological types. Second, the colors of earlier-type galaxies can be fitted at model ages $\lesssim 15$ Gyr, whereas late type Spirals seem better represented by older models ($\gtrsim 15$ Gyr). This result would easily be disproved if the reddening corrections applied to Spirals in the sample (Aaronson 1978 and references therein) had only slightly been underestimated.

It is worth recalling that some galaxies have colors which cannot be fitted by the simple models in Figure 11. For instance, the so-called blue compact dwarf galaxies may result from a recent star burst superimposed on an old stellar population (Thuan 1983). These galaxies have $V-K$ colors ranging between 0 and 3 (and associated $U-V$ colors between -0.5 and 0.5) depending on the ratio of the mass of stars formed during the recent burst to the mass of the old population. Fitting these colors would require to also model the light of the underlying population (several blue compact dwarf galaxies may also be metal deficient). The above results suggest that since isochrone synthesis models can reproduce accurately the photometric evolution of star bursts as well as that of older galaxies, they are a powerful mean to investigate galaxies with any peculiar star formation history.

V. SUMMARY AND CONCLUSION

We have introduced the isochrone synthesis method to population synthesis of galaxies. This method allows us to compute accurate distributions of stars in the theoretical CMD for any stellar population and to thereby circumvent the problems faced by earlier techniques (conventional population synthesis, fuel consumption theorem). To optimize our models, we have compiled a set of evolutionary tracks (for solar abundances) by assembling updated stellar models in good agreement with the observations. We have avoided to rely on controversial models of TP-AGB stars by deriving semi-empirically the positions of these stars in the theoretical CMD. The resulting tracks extend from the ZAMS up to the beginning of the white-dwarf cooling sequence. After comparing our isochrone synthesis models with models based on the fuel consumption theorem and computed with the same library of tracks, we conclude that the latter are a reasonable although misleading approximation of population synthesis. Indeed, such models underestimate by 20%–40% the age of a stellar system inferred from the distribution of the bolometric luminosity among the various stellar components. Earlier results obtained with the fuel consumption theorem (Renzini and Buzzoni 1986) are superseded by the new library of tracks.

We have compared the predictions of various isochrone synthesis models with observational data. The predicted contribution of bright AGB stars to the integrated bolometric light of a burst stellar population is remarkably close to that observed by Frogel *et al.* (1990) in a sample of Magellanic Clouds clusters. Also, a single burst model with the Salpeter IMF reproduces well the broad-band $UBVK$ colors of a representative sample of LMC clusters with ages between 1×10^7 and $\lesssim 4 \times 10^9$ yr. Given that any SFR is expandable in series of bursts, this implies that the isochrone synthesis models can be used reliably in studies of more complex populations. We have computed a series of models with star formation time scales from a few times 10^8 yr to infinity (constant SFR) and the Salpeter IMF. We find that the range of UVK colors of these models after $\gtrsim 10$–13 Gyr coincides with the spread of colors observed in present-day galaxies of Hubble types E to Sd. All models have the UVK colors of an average Im galaxy around 1 Gyr. The inferred dependence of star formation history on morphological type is consistent with that determined elsewhere from spectrophotometric studies of nearby galaxies. Hence, the isochrone synthesis models can reproduce the observed colors of stellar populations of ages from a few times 10^7 yr to a Hubble time. We consider these successful comparisons as an evidence for the appropriateness of the set of evolutionary tracks and of the isochrone synthesis method.

Despite the relative success of the models presented in this paper, a few points may be raised that need further improvement. In particular, the present models are for solar metallicity only. Although evolutionary tracks for other metallicities are available, the crucial lack of photometric calibrations and detailed spectral information for nonsolar abundances are a serious handicap for their implementation in population synthesis models. Ideally, a population synthesis model should also include exotic objects like binaries (Greggio and Renzini 1990), supernovae, a nebular component, internal dust, etc. Unfortunately, the implications of these missing components on the integrated light of a stellar population are far from understood and rely on ill-known parameters. Work is in progress, however, to include (even roughly) some of them in the isochrone synthesis models.

Many people have expressed interest in this project and provided interesting discussions. In particular we are grateful to Mike Fall for helpful comments on the paper. G. Meynet and E. Bica made helpful suggestions on an early draft. We thank A. Maeder and C. Chiosi for enlightening discussions on stellar evolution, and David Koo and Rosie Wyse for encouragement in updating stellar population synthesis models. S. C. thanks the French Ministère de la Recherche et de la Technologie for partial support. G. B. A. acknowledges ample financial and computer support from STScI during various stages of this project.

APPENDIX

We describe here the procedure adopted to complement the MM tracks of stars less massive than $\lesssim 6.6\ M_\odot$ for the late evolutionary stages. We proceed in three steps. For low-mass stars, we complement the evolution beyond the He-Flash until the end of the E-AGB phase with updated stellar models. For both low- and intermediate-msss stars, we evaluate the location of the TP-AGB in the theoretical CMD using a semi-empirical approach. We then include the PAGB evolution down to the beginning of the white-dwarf cooling sequence.

a) Core-He Burning of Low-Mass Stars

The evolution of stars initially less massive than $M_{\rm HeF}$ and which undergo degenerate central He-ignition has been extensively studied (Iben and Rood 1970; Sweigart and Gross 1976; Renzini 1977; Caputo, Castellani, and Wood 1978; Castellani *et al.* 1985; Bressan *et al.* 1986; Seidel, Demarque, and Weinburg 1987). Despite the very different input physics of the various models (none of which identical to that used by MM), the resulting tracks in the theoretical CMD agree within $\Delta \log (T_{\rm eff}) \lesssim 0.01$ and $\Delta \log (L/L_\odot) \lesssim 0.05$. From a population synthesis point of view these variations are negligible as compared to the precision of the stellar photometric data. Of more significance is the variation of the duration of the CHeB phase among the different models. The comparison of models of appropriate metallicity ($Z \approx 0.001$) with star counts in globular clusters (Buzzoni *et al.* 1983) is in favor of the recent calculations of Bressan *et al.* (1986; see their Table 3). Thus, we use evolutionary tracks computed according to the same prescription as in Bressan *et al.* (1986) but for solar metallicity (Chiosi 1989) in order to describe the evolution of stars $\leq 1.85\,M_\odot$ from the zero-age horizontal branch up to the end of the E-AGB phase. These models favor a somewhat higher efficiency of convective overshooting than MM.

b) TP-AGB Evolution of Low- and Intermediate-Mass Stars

Stars at the beginning and at the end of the TP-AGB have been observationally identified as, respectively, Miras and OH/IR variables (§ II of this paper, Bedijn 1988). Using observed samples of galactic (solar-metallicity) stars and little input physics, we now determine the loci of Miras and OH/IR variables in the theoretical CMD for different progenitor masses, as well as the relative duration of the two phases. We use this information to complement the stellar evolutionary tracks of low- and intermediate-mass stars. In the following, the effective temperature of a TP-AGB star is that of the central object embedded in the circumstellar shell.

i) *Effective Temperatures and Progenitor Masses of Observed TP-AGB Stars*

Herman and Habing (1985) have determined the effective temperatures and ZAMS progenitor masses of $\sim$40 galactic OH/IR stars from a flux-density limited sample in the Baud *et al.* (1979) 1612 MHz survey. They combined accurate measurements of the pulsation periods and period-averaged bolometric luminosities (Herman *et al.* 1986) with theoretical relationships. Given the controversy about models of TP-AGB stars, we feel necessary to recompute the temperatures and progenitor masses of the OH/IR stars by estimating their dependence on the few theoretical relationships involved in their determination. Herman and Habing (1985) and Herman *et al.* (1986) also collected data for a smaller sample of Mira variables which can be used to derive in the same way their temperatures and progenitor masses.

The effective temperature of an OH/IR star can be determined analytically from its observed mass and luminosity, the mass being inferred from the pulsation period (Fox and Wood 1982). Herman and Habing (1985) used the relationship of Becker and Iben (1979) to compute the temperatures of their sample stars in this way. Other estimates of $\log T_{\rm eff}$ can be computed using different expressions given elsewhere (Iven and Truran 1978; Renzini and Voli 1981; Lattanzio 1986). In all cases, we find that the mean over the sample stars of the difference in $\log T_{\rm eff}$ with Becker and Iben's value is less than 0.06, and the standard deviation less than 0.03. This scatter is roughly of the same order as the photometric resolution of our isochrone synthesis models. Hence, effective temperatures estimated from the observed masses and luminosities seem satisfactory.

The ZAMS–progenitor masses of OH/IR stars can be estimated in several ways. Following Herman and Habing (1985) we compute the progenitor mass as an average of three determinations. Two methods, one of which purely empirical, involve the observed expansion velocity of the shell and do not depend on the uncertainties of the stellar evolution theory (see their paper for detail). The ZAMS–progenitor mass can also be determined indirectly from the observed luminosity. Herman and Habing (1985) used the luminosity/core-mass relationship from Wood and Zarro (1981), and the core-mass/ZAMS-mass relationship from Iben and Truran (1978). Alternative expressions of the luminosity/core-mass relationship include those of Paczyński (1970), Iben (1977), Renzini and Voli (1981), and Lattanzio (1986). In all cases, the mean over the sample stars of the relative difference with the ZAMS masses computed using Wood and Zarro's relation never exceeds 4%, with a standard deviation less than $\sim$2.5%. Here, and in the following, the quoted errors refer to the ZAMS–mass averaged over the three determinations mentioned above. Using the core-mass/ZAMS–mass relationship inferred from Figure 13 of Bertelli, Bressan, and Chiosi (1985) instead of that from Iben and Truran (1978) yields a mean relative difference in ZAMS masses $\lesssim 3\% \pm 2\%$ for lower-mass stars, reaching $\lesssim 9\% \pm 1\%$ for the more massive intermediate-mass stars (roughly between 3 $M_\odot$ and $\gtrsim 6\,M_\odot$). The larger discrepancy for higher mass stars is due to the large amount of overshooting used by Bertelli *et al.* (1985), the effect of which increases with the ZAMS mass (e.g., Renzini and Voli 1981). As emphasized by MM, the efficiency of overshooting is more likely to be only 25% of the value advocated by Bertelli *et al.*, so that the masses obtained with Iben and Truran's relation should be more reliable. The final ZAMS–progenitor masses of the sample OH/IR stars range between $\lesssim 1\,M_\odot$ and $\gtrsim 6\,M_\odot$.

Herman and Habing (1985) and Herman *et al.* (1986) also determined the pulsation periods and period-averaged bolometric luminosities of nine Mira variables. We have derived the effective temperatures and ZAMS-progenitor masses of these stars in the same way as for the OH/IR stars. However, Mira variables have thinner circumstellar shells so that OH masering is weak or absent, and the expansion velocity of the shell cannot be measured. Therefore, the ZAMS–progenitor masses in this case were inferred from the core-mass/ZAMS–mass relationship only. Even though only nine Miras were studied, the range of ZAMS–progenitor masses expands from $\sim 1.3\,M_\odot$ to $\sim 5\,M_\odot$ so that enough information is available to build the tracks.

ii) *Inclusion of TP-AGB Stars in the Tracks Library*

Figure 12 shows the resulting positions of Miras and OH/IR stars in the theoretical CMD. We note that for the more massive intermediate-mass stars ($\gtrsim 2\,M_\odot$), the lower TP-AGB is close to the end of the E-AGB computed by MM. We then complement each stellar evolutionary track below 6.6 $M_\odot$ with two points corresponding respectively to the beginning (Mira phase) and to the end (OH/IR phase) of the TP-AGB. For tracks above 1.7 $M_\odot$, the effective temperature and bolometric luminosity of the lower

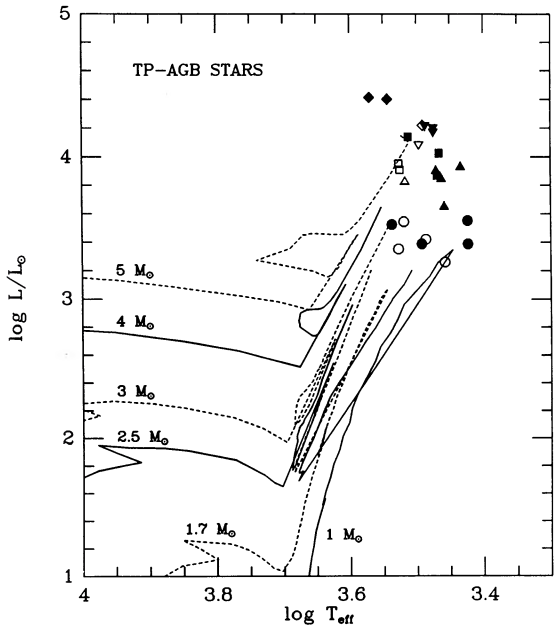

FIG. 12.—Positions in the theoretical CMD of observed galactic TP-AGB stars with different ZAMS–progenitor masses. Open symbols refer to the beginning (Miras) of the TP-AGB. Filled symbols refer to the end (OH/IR) of the TP-AGB. The stellar evolutionary tracks (up to the end of the E-AGB) are from the sources referenced in the text. To avoid confusion, only a few tracks have been plotted, using alternatively solid lines and dashed lines. Only TP-AGB stars whose progenitor masses were close to the ZAMS masses on these tracks are shown (5 $M_\odot$: *diamonds*; 4 $M_\odot$: *upside down triangle*; 3 $M_\odot$: *squares*; 2.5 $M_\odot$: *triangles*; $\leq 1.7\ M_\odot$: *circles*).

TP-AGB is computed by averaging over the temperatures and luminosities of Miras with progenitor masses close to the initial mass on the track (ZAMS). For stars below 1.7 $M_\odot$, owing to the width of the RGB and the scatter in the observed temperatures (see Fig. 12), the luminosity in the lower TP-AGB phase is inferred from the Miras sample while the temperature is taken the same as at the tip of the RGB (both $T_{\rm eff}$ and L are taken at the He-Flash for stars $< 1.3\ M_\odot$ since no Miras have been observed). This is supported by the observational evidence that the AGB of low-mass stars is a continuation of the RGB (e.g., Iben and Renzini 1983). We use the same procedure to locate the stars on the upper TP-AGB from the sample of OH/IR variables.

We infer the durations of the lower and upper TP-AGB phases from the model of AGB evolution developed by Bedijn (1988). His model describes the combination of stellar pulsations with radiation pressure on the shell material, and their control of mass loss. One attractive feature of such a model is that it allows several comparisons with the observations. Models that predict the evolution of the central object only are more difficult to test. Bedijn's model reproduces acceptably the observed statistical properties of local Miras and OH/IR variables (period distribution of classical Miras, OH 1612 MHz luminosity function including both Miras and OH/IR stars). The various other theoretical time scales proposed in the literature (Becker and Iben 1979; Renzini and Voli 1981; Boothroyd and Sackmann 1988) suffer a crucial lack of observational support.

c) *PAGB Evolution of Low- and Intermediate-Mass Stars*

At the end of the AGB, low- and intermediate-mass stars lose their envelope, leading to the formation of a PN. The central stars of PNs have fading times which strongly depend on the core mass at PN ejection (Iben and Renzini 1983; Schönberner 1983). Current estimates of the upper core-mass limit for the bright nucleus to remain after the nebula has dispersed roughly agree on $M_c \lesssim 0.6\ M_\odot$ (Iben and Renzini 1983; Spergel *et al.* 1983; Schönberner 1983, 1986). Using the core-mass/ZAMS–mass relationship of Iben and Truran (1978), this corresponds to a progenitor mass $\lesssim 2.5\ M_\odot$. Hence, we do not follow the evolution of stars initially more massive than 2.5 $M_\odot$ beyond the TP-AGB phase since they never appear as bare PN nuclei. Schönberner (1983) carried out detailed calculations of the PAGB evolution of stars with lower ZAMS masses, and core masses 0.565 $M_\odot$ and 0.546 $M_\odot$. His models were questioned later (Iben 1984; Wood and Faulkner 1986) on the ground that PAGB stars may leave the AGB during He-burning instead of quiet H-burning as he advocated, leading to important differences in their evolution. Subsequent observations of a large sample of PNs (Schönberner 1986) seem to favor the earlier models of Schönberner (1983).

One can arrange the OH/IR stars in the Herman and Habing (1985) sample with ZAMS–progenitor masses lower than 2.5 $M_\odot$ into two mass groups. Those with progenitor masses lower than $\lesssim 1.5\ M_\odot$ turn out to have a mean core mass $\approx 0.536 \pm 0.020\ M_\odot$, while those with progenitor masses in the range $1.5\ M_\odot \lesssim M_c \lesssim 2.56\ M_\odot$ have a mean core mass $\approx 0.566 \pm 0.050\ M_\odot$. We therefore assume that stars with ZAMS masses $< 1.5\ M_\odot$ have a PAGB evolution similar to the $M_c = 0.546\ M_\odot$ model of Schönberner (1983), while stars with ZAMS masses in the range $\gtrsim 1.5\ M_\odot$ to $\lesssim 2.5\ M_\odot$ behave as his $M_c = 0.565\ M_\odot$ model. We assume that during the first 3×10^4 yr of its PAGB evolution (i.e., the typical "observed" PN lifetime, Iben and Renzini 1983), a PAGB star does not contribute to the galactic spectrum since its envelope has not yet dispersed.

REFERENCES

Aaronson, M. 1978, ApJ, 221, L103
Arimoto, N., and Yoshii, Y. 1986, A&A, 164, 260
Baud, B., Habing, H. J., Matthews, H. E., and Winnberg, A. 1979, A&AS, 36, 193
Becker, S. A. 1981, ApJS, 45, 475
Becker, S. A., and Iben, I., Jr. 1979, ApJ, 232, 831
Becker, S. A., and Mathews, G. J. 1983, ApJ, 270, 155
Bedijn, P. J. 1988, A&A, 205, 105
Bertelli, G., Bressan, A., and Chiosi, C. 1985, A&A, 150, 33
Bica, E. 1990, preprint
Böhm-Vitense, E. 1972, A&A, 17, 335
Boothroyd, A. I., and Sackmann, I. J. 1988, ApJ, 328, 653
Bressan, A., Bertelli, G., and Chiosi, C. 1986, MSAI, 57, 411
Bruzual A., G. 1983, ApJ, 273, 105
Burstein, D., Bertola, F., Buson, L. M., Faber, S. M., and Lauer, T. R. 1988, ApJ, 328, 440
Buzzoni, A. 1990, ApJS, 71, 817
Buzzoni, A., Fusi Pecci, F., Buonanno, R., and Corsi, C. E. 1983, A&A, 128, 94
Caputo, F., Castellani, V., and Wood, P. R. 1978, MNRAS, 184, 377
Castellani, V., Chieffi, A., Pulone, L., and Tornambé, A. 1985, ApJ, 294, L31
Chambers, K. C., and Charlot, S. 1990, ApJ, 348, L1
Chiosi, C. 1989, private communication
Chiosi, C., and Maeder, A. 1986, ARAA, 24, 329
Chiosi, C., Bertelli, G., and Bressan, A. 1988, A&A, 196, 84
Cohen, J. G. 1982, ApJ, 258, 143
Dyck, H. M., Zuckerman, B., Leinert, Ch., Beckwith, S. 1974, ApJ, 189, 89
Elson, R. A. W., and Fall, S. M. 1985, ApJ, 299, 211
———. 1988, AJ, 96, 1383
Flower, P. J. 1977, A&A, 54, 31
Fox, M. W., and Wood, P. R. 1982, ApJ, 259, 198
Frogel, J. A., Mould, J., and Blanco, V. M. 1990, ApJ, 352, 96
Gallagher, J. S., Hunter, D. A., and Tutukov, A. V. 1984, ApJ, 284, 544
Greggio, L., and Renzini, A. 1990, ApJ, in press
Guiderdoni, B., and Rocca-Volmerange, B. 1987, A&A, 186, 1
Herman, J., and Habing, H. J. 1985, PR, 124–4, 255
Herman, J., Burger, J. H., and Phennix, W. H. 1986, A&A, 167, 247
Iben, I., Jr. 1967, ARAA, 5, 571
———. 1974, ARAA, 12, 215
———. 1977, ApJ, 217, 788
———. 1984, ApJ, 277, 333
Iben, I., Jr., and Renzini, A. 1983, ARAA, 21, 271
Iben, I., Jr., and Rood, R. T. 1970, ApJ, 161, 587
Iben, I., Jr., and Truran, J. W. 1978, ApJ, 220, 980
Johnson, H. L. 1966, ARAA, 4, 193
Joseph, R. 1990, preprint
Kennicutt, R. C. 1983, ApJ, 272, 54
Lattanzio, J. C. 1986, ApJ, 311, 708
Maeder, A. 1976, A&A, 47, 389
———. 1989, preprint
———. 1990, preprint
Mader, A., and Meynet, G. 1988, A&AS, 76, 411
———. 1989, A&A, 210, 155 (MM)
Nomoto, K. 1987, ApJ, 322, 206
Paczyński, B. 1970, ActaA, 20, 47
Persson, S. E., Aaronson, M., Cohen, J. G., Frogel, J. A., and Matthews, K. 1983, ApJ, 266, 105
Reid, N., Tinney, C., and Mould, J. 1990, ApJ, 348, 98
Renzini, A. 1977, in Advanced Stages of Stellar Evolution, ed. P. Bouvier, and A. Maeder (Geneva: Geneva Obs), p. 151
———. 1981, AnnPhysFr, 6, 87
———. 1987, A&A, 188, 49
———. 1988, in Evolutionary Phenomena in Galaxies, ed. J. E. Beckman and B. E. J. Pagel (Cambridge: Cambridge Univ. Press), p. 422
Renzini, A., and Buzzoni, A. 1983, MSAI, 54, 739
———. 1986, in Spectral Evolution of Galaxies, ed. C. Chiosi and A. Renzini (Dordrecht: Reidel), p. 195
Renzini, A., and Voli, M. 1981, A&A, 94, 175
Salpeter, E. E. 1955, ApJ, 121, 161
Scalo, J. M. 1986, FunCosP, 11, 1
Schönberner, D. 1983, ApJ, 272, 708
———. 1986, A&A, 169, 189
Searle, L., Wilkinson, A., and Bagnuolo, W. G. 1980, ApJ, 239, 803
Seidel, E., Demarque, P., and Weinberg, D. 1987, ApJS, 63, 917
Spergel, D. N., Giuliani, J. L., Jr., and Knapp, G. R. 1983, ApJ, 275, 330
Sweigart, A. V., and Gross, P. G. 1976, ApJS, 32, 367
Thuan, T. X. 1983, ApJ, 268, 667
Tinsley, B. M. 1980, ApJ, 241, 41
van den Bergh, S. 1981, A&A, 46, 79
Weidemann, V., and Koester, D. 1984, A&A, 121, 77
Wood, P. R., and Faulkner, D. J. 1986, ApJ, 307, 659
Wood, P. R., and Zarro, D. M. 1981, ApJ, 247, 274
Woosley, S. E., and Weaver, T. A. 1986, ARAA, 24, 205
Wyse, R. F. G. 1985, ApJ, 299, 593
Zhou, K., Hao, Y., Chen, P., Zhang, Y., and Gao, M. 1986, ApSpaceS, 107, 373

GUSTAVO BRUZUAL A.: Centro de Investigaciones de Astronomía (CIDA), AP 264, 5101-A Mérida, Venezuela

STÉPHANE CHARLOT: Space Telescope Science Institute, 3700 San Martin Drive, Baltimore, MD 21218